# Injection locking of a long-pulse relativistic magnetron

S.C. Chen, G. Bekefi, and R.J. Temkin

Plasma Fusion Center
Massachusetts Institute of Technology
Cambridge, MA 02139

## ABSTRACT

We report the injection locking results of a long-pulse (200–400 ns) high power (20–30 MW) relativistic magnetron. The cold-cathode magnetron structure is driven by a high power modulator to generate S-band output at 3.3 GHz. Phase-locking with reproducible locked angle is achieved with an injection power ratio as low as 1:200. The locked states are phase stable to within ±3° during the pulse. Repetition-rated operation at 5 Hz produces average powers higher than single shot systems. Phase locking physics is studied by parametrically scanning the injection frequency and varying the injection power. Important effects due to frequency pushing are identified. The measured locking bandwidth agrees well with a theory which takes into account frequency pushing effects. The measured dependence of final locked phase on injection frequency and injection power also agrees well with theory.

## 1. INTRODUCTION

Phase-locking of a high power relativistic magnetron oscillator has been a subject of intensive experimental [1-5] and theoretical research. [6-9] Phase locking through the injection of an external low power reference signal has the following advantages which are important in realizing a large array of locked oscillators. First, the same phase locking physics applies to all the master-slave pairs and to the whole phase-locked array. No additional complication arises from the simple nonreciprocal coupling. Second, interactive control of phase and frequency, if necessary, can be effectively accomplished by adjustments made at very low power levels. Third, several high power oscillators can share the same low power driver, which is usually simple and available at low cost. Injection locking, however, requires high power oscillators with good mode and frequency stability, and with a pulse length longer than the phase-locking time.

This paper describes the operation of such a long-pulse relativistic magnetron oscillator system and its injection-locking. Section 2 describes the apparatus used in the experiment. Section 3 discusses the general operating characteristics of the free running relativistic magnetron (3.1) and the results of the phase locking experiment (3.2). Section 4 summarizes the main results of the phase locking study.

## 2. APPARATUS

The nonlinear interdependence of the magnetron dynamic impedance and diode voltage determines the main operating characteristics of cold-cathode relativistic magnetrons. As a result, the RF output features (power, efficiency, pulse length and mode purity) depend on the choice of magnetron diode geometry, cathode (emission) materials, and power supply impedance. [1] It was found that a high vacuum environment and a clean anode surface are essential for obtaining RF pulse lengths longer than 250 ns. For higher power and longer pulse operations, the experiment has been completely redesigned and rebuilt. Better diagnostics and higher vacuum are obtained, and the impedance mismatch between the magnetron diode and the power supply is minimized.

The schematic of the system is shown in figure 1. The transformer-based high power modulator produces up to 500 MW, 2 $\mu$s pulses with a repetition rate of 5 Hz. [10] The high voltage pulses are delivered through the cathode shank to the magnetron diode. The relativistic magnetron diode is located at the center of the bore of a superconducting magnet capable of generating uniform DC fields up to 22 kG. The vacuum system is evacuated through a pumping

port. Microwave output is extracted radially in waveguide through the radial access holes in the superconducting magnet.

Major improvements are described in the following. A bakeable metal-ceramic high voltage insulator, originally designed for a SLAC electron gun, is installed to replace the plastic voltage hold-off section for long pulse operation under high vacuum. The vacuum system has been upgraded with high vacuum flanges and evacuated by a turbo pump. The base pressure obtained is $1 \times 10^{-7}$ Torr. A vacuum cross at the end of the system provides additional diagnostic and view ports. The operating voltage is measured by a capacitive voltage divider in the modulator tank. The total and axial currents are measured by a current viewing resistor and an imbedded Rogowski coil, respectively. The pulse transformer in the modulator has been modified to contain a multi-tab secondary, which provides four step-tuned transforming ratios: 1:5, 1:8, 1:12, and 1:20. The feature enables us to vary the impedance of the modulator to match that of the relativistic magnetron (RM).

The experimental parameters are listed in Table I. The magnetron diode (SM2) has a large A-K gap (1.35 cm) to prevent gap-closure and to enhance the power handling capability of the structure. The SM2 structure is shown in figure 2. A thick velvet washer (5 mm) is chosen for the phase locking experiment. Thicker cathodes have longer lifetimes and sustain the 2D-mode structure better than thin washers.

The following equipments and components were calibrated systematically before and after the experiment: current and voltage probes, scopes, gauss meters, RF cables, connectors, circulator, isolators, directional couplers, attenuators, frequency counter, wavemeter, and phase detector. Four channels of 100 MHz digital scopes are used in addition to the analog scopes at 400 MHz and 200 MHz.
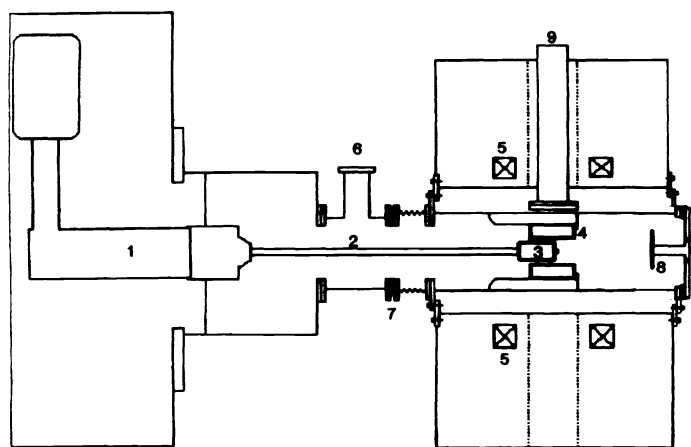


**Figure 1**

Schematic of the relativistic magnetron system. The modulator (1) output is delivered through the cathode shank (2) to the magnetron cathode (3). The anode (4) is held at ground potential to maintain the voltage drop across the anode-cathode gap. The relativistic magnetron diode is located in the center of the bore of a superconducting magnet (5). The vacuum system is evacuated through a pumping port (6). The total current is measure with a Rogowski coil ; the axial current is measured with a current viewing resistor (8). Microwave output is extracted radially in waveguide through the radial access holes (9) in the superconducting magnet. The injection signal is launched through the same access hole into the magnetron interaction region.

### Table I.  Experimental Parameters

**Relativistic Magnetron**

| | |
|---|---|
| Anode radius | 1.85 cm |
| Cathode radius | 0.5 cm |
| Vane radius | 3.68 cm |
| Vane # | 6 |
| Vane angle | 20° |
| Cathode length | 5 mm (thick washer) velvet |
| Natural frequency | 3.292 GHz |
| Voltage | 220 kV |
| Current | 700 A |
| Peak power | 30 MW |
| Pulse length | 400 ns |

**Driver Magnetron**

| | |
|---|---|
| Peak power | 1 MW |
| Pulse length | 1 $\mu$s |
| Frequency | 3.1 – 3.47 GHz |

# 3. EXPERIMENTAL RESULT

## 3.1 Operating characteristics

The general operating characteristics of the cold-cathode relativistic magnetron (RM) is described next. Figure 3 shows the time dependence of output microwave and the corresponding magnetron voltage. The microwave duration ranges from 200 to 400 ns. The spiky feature in the output power is due to the voltage fluctuations caused by the unstable cold-cathode emission process. The output power fluctuation is reduced in the injection phase-locked case (see figure 5) to be described in the next section. The magnetron voltage is about 200 kV across the A-K gap, and the pulse width (FWHM) is about 1 $\mu$s. The impedance of the magnetron diode varies slowly with time, and no signs of impedance collapse (on the fast time scale) are observed. The axial current waveshape, in general, follows that of the voltage pulse, and the magnitude is about half the total current. The difference of total and axial current is the radial current, which is responsible for the magnetron gain. Microwaves are generated at the onset of the radial current, which is about 300–400 A. Typical peak powers are between 20 and 30 MW. The efficiency, namely the output power normalized to the total electron beam power, is about 16 percent. It is believed that the efficiency can be improved by reducing the axial current. The system can run rep-rated at 5 Hz without degradation in output power or in pulse length. The long washer cathode lasted for more than 5000 shots.

## 3.2 Phase locking result

The layout of the phase-locking experiment is shown schematically in figure 4. Microwave radiation is extracted from the interaction region through a high power circulator with 20 dB isolation. The power from the tunable 1 MW RF driver is injected through the same circulator into the main oscillator. The signals from the driver and the relativistic magnetron are monitored for power, frequency, and relative phase evolution. A 20 dB isolator is placed between the driver and the circulator so that the overall isolation is 40 dB. The isolation prevents the driver from being locked by RM's leakage power.



Figure 2 Photograph of the SM2 magnetron. The structure has a large A-K gap (1.35 cm) to prevent gap-closure and to enhance power handling capability. Thicker cathodes, 5 mm, have longer lifetimes and sustain the 2D-mode structure better than thin washer cathodes.
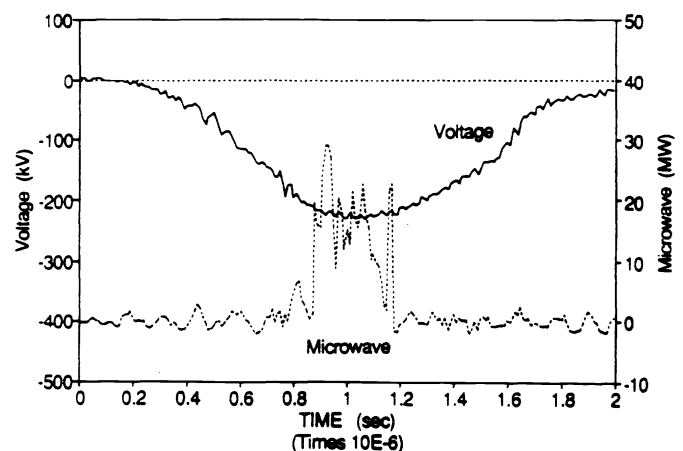


Figure 3

Operating characteristics of a free-running SM-2 magnetron. Time dependence of output power and the corresponding magnetron voltage. The length of the 20-30 MW microwave pulse ranges from 200 to 400 ns. The magnetron voltage is about 200 kV across the A-K gap, and the pulse width (FWHM) is about 1 $\mu$s. The impedance of the magnetron diode varies slowly with time, and no signs of impedance collapse are observed.

The phase detector used is the Anaran phase discriminator 2A0750 which has a high sensitivity and a 30 dB dynamic range. The video amplifier gain is about 200 and the bandwidth is larger than 10 MHz. The linearity of the relative phase output is measured to be better than 1° at the operating frequency 3.3 GHz.

Clear signs of phase locking are observed under the most favorable conditions: full power (1 MW) injection at the RM's free-running frequency, and the injection power turns on before the onset of RM power output and stays on during the RM microwave pulse. Figure 5 is an example of such a shot: The driver signal $P_i$ (middle trace) is monitored before injection into the circulator. The upper trace shows the high power RF from the RM riding on top of a low power injection plateau. The injection plateau is formed by the driver power after being injected into and subsequently circulated out of the RM interaction region. The signal is sampled right before the high power load (see figure 4) and is marked as $P_0$. The low power plateau is a convenient signature for confirming power levels and for identifying phase-locked states. The low power injection plateau is absorbed by the high power load and does not cause reverse locking of the driver. The time delay between the driver signal and the low power plateau signal is consistent with the signal transit time in the long RF transport waveguide.
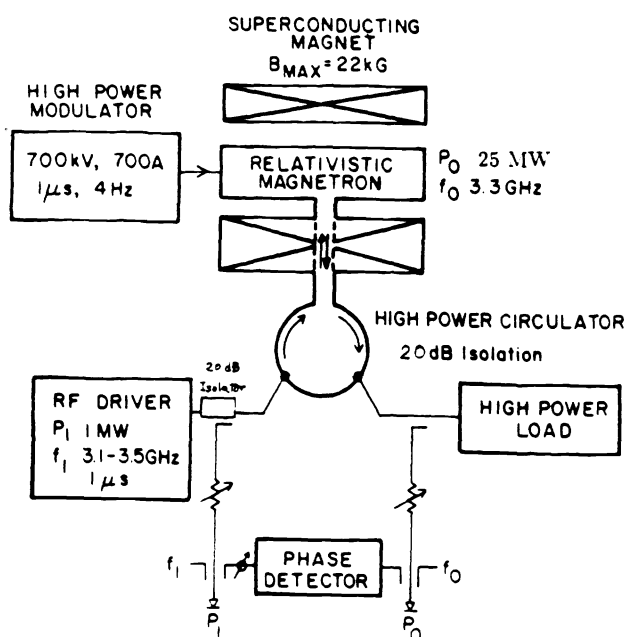


Figure 4

Schematic of the phase-locking experiment. Microwave radiation is extracted from the interaction region through a high power circulator with 20 dB isolation. The power from the tunable 1 MW RF driver is injected through the same circulator into the main oscillator. The signals from the driver and the relativistic magnetron are monitored for power, frequency, and relative phase evolution. A 20 dB isolator between the driver and the circulator increases the overall isolation to 40 dB. The isolation prevents the driver from being locked by RM's leakage power.
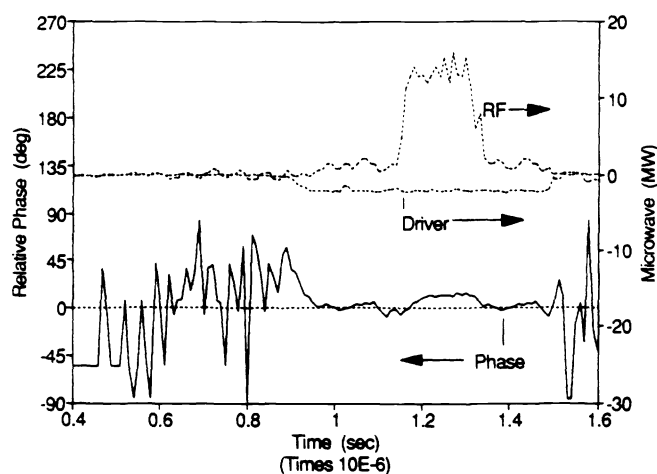


Figure 5 Example of a phase-locked shot. The middle trace is the driver signal. The upper trace shows the high power RF from the RM riding on top of a low power injection plateau. The injection plateau is formed by the driver power after being injected into and subsequently circulated out of the RM interaction region. The bottom trace is the time evolution of the relative phase. During the absence of the RM signal (in the time interval between 0.9 and 1.1 $\mu$s) the phase detector measures the constant relative phase (at 0°) between the driver signal and its own image – the low power plateau. When the RM turns on at 1.15 $\mu$s, the relative phase locked to a new angle at 12 °. This locked phase angle is reproducible from shot to shot. The relative phase relaxes back to 0° when the RM is off.

The bottom trace in figure 5 shows the evolution of the relative phase. During the absence of the RM signal (for example, in the time interval between 0.9 and 1.1 $\mu$s) the phase detector measures the relative phase between the driver signal and its own image – the low power plateau. The result is a relative phase constant in time. We use this as a reference state at 0°. When the RM turns on at 1.15 $\mu$s, the relative phase is pulled to a new angle at 12 °. This new phase angle is reproducible from shot to shot and defines a phase locked state which relaxes back to the reference state at 0° when the RM is off (see figure 5).

Under these most favorable conditions for phase locking, namely full power injection at zero frequency difference, the stability and reproducibility of the phase-locked states are measured. By using a stringent criterion of ±3° to define the phase-locked states, typically the locked duration is between 100 and 300 ns. Relaxing the ±3° phase locking criterion leads to longer locked duration. The shot-to-shot reproducibility of the final locked phase angle is better than ±2°.

Phase locking is also confirmed by frequency spectrum measurements. The frequency spectra of the RM output with and without injection are measured with a SAW device running with a 300 ns gate pulse. The free-running RM central frequency is at 3.292 GHz with a FWHM bandwidth of 20 MHz. The shot-to-shot frequency variation is ±10MHz. The frequency spectrum of RM under full power injection showed clear frequency-locked features: the central frequency is stabilized with almost no shot-to-shot variation; the bandwidth is narrowed down from ±10 MHz to ~6 MHz, close to the driver bandwidth.

Parametric phase-locking studies are carried out by scanning the injection frequency and varying the injection power. The phase-locking results are analyzed and compared with theory next.

The results of a large number of experiments involving various injection frequencies (ranging from -10 MHz to 10 MHz) and injection power ratios (ranging from 1:1000 to 1:10) are compiled in figure 6. The solid squares in the figure stand for the cases phase-locked states are identified. The blank squares represent those cases when no phase-locking occurs.
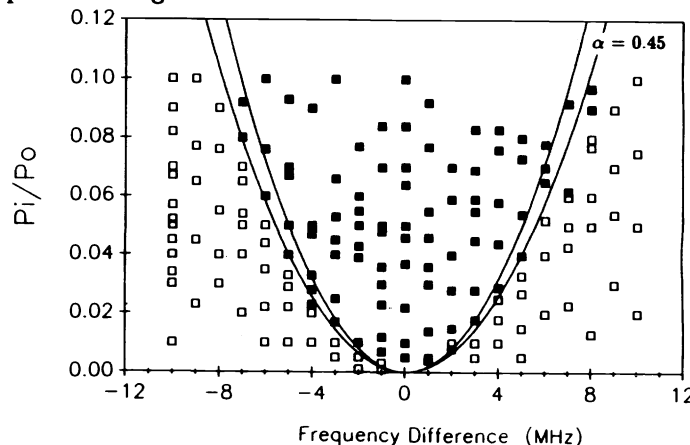


Figure 6

Map of the phase-locking zone. The horizontal axis is the frequency difference between the driver and the free-running relativistic magnetron. The vertical axis is the injection power ratio. The solid squares stand for the cases phase-locked states are identified. The blank squares represent cases when no phase-locking occurs. The two solid curves are the locking zone boundaries predicted by (1) the Adler's condition with frequency pushing effect correction and (2) the Adler's condition alone. The data points are consistent with the theory curve with a pushing parameter $\alpha$ of 0.45.
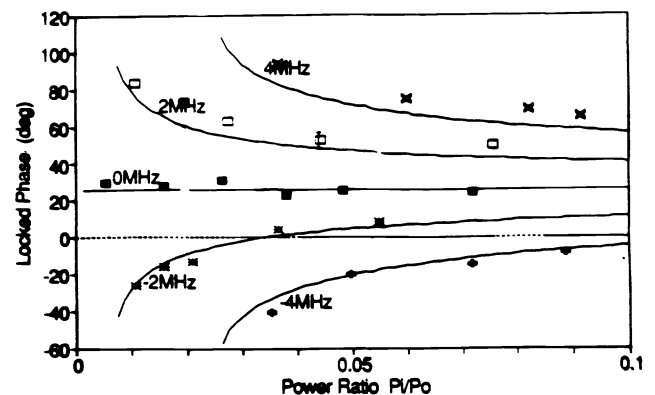


Figure 7

The dependence of the final locked-phase on the injection power and injection frequency difference. The cases for 5 injection frequencies are shown for various injection power ratios. The data points agree well with the theory with a frequency pushing parameter $\alpha$ of 0.45.

Frequency pushing effect, namely the variation of frequency of oscillation with electrode current, was studied theoretically and found to affect the phase-locking behaviour in nonlinear oscillators provided the magnitude of the frequency pushing is large enough.[6] A magnetron-specific phase-locking model was developed in reference 6 using the standard equivalent-circuit approach which takes into account the frequency pushing effect. The model predicts a locking-bandwidth wider than that in conventional locking theory

$$\Delta\omega \leq \frac{\omega_0}{2Q \cdot cos\alpha} \cdot \sqrt{\frac{P_i}{P_o}}.$$

In the equation, $\Delta\omega$ is the locking frequency range, $\omega_0$ is the free-running oscillator frequency, $\alpha$ is the frequency pushing parameter,[6] and $P_o$ and $P_i$ are the oscillator output and input power, respectively. The $1/cos\alpha$ factor is the attributed to the frequency pushing effect in RMs.

The two solid curves in figure 6 are the locking zone boundaries predicted by (1) the Adler's condition with frequency pushing effect correction and (2) the Adler's condition alone. The data points are consistent with the theory curve described by the above equation with a pushing parameter $\alpha$ of 0.45.[6]

The magnitude of frequency pushing is also confirmed in an independent measurement of the final phase. In figure 7, the dependence of the final locked-phase on the injection power and frequency is mapped out. The cases for 5 injection frequencies ( -4MHz, -2MHz, 0MHz, 2MHz, and 4MHz) are shown for various injection power ratios (1:1000 to 1:10). Again, the data points agree well with the theory with a frequency pushing parameter $\alpha$ of 0.45.

## 4. CONCLUSION

We have phase locked an S-band (3.3 GHz) long-pulse high power relativistic magnetron oscillator (400 ns at 25 MW) by external injection (20 kW – 1 MW). A reproducible final phase-locked angle is achieved with an injection power ratio as low as 1:200. The phase stability of the phase-locked states is $\pm 3°$ degrees throughout the 300 ns pulse.

Parametric study of the phase-locked states reveals the importance of frequency pushing effect in phase-locking. The measured locking bandwidth agrees well with the theory which takes into account the frequency pushing effect. The measured dependence of final locked phase on $\Delta\omega$ and $P_i/P_o$ also agrees well with theory.

We have identified the relativistic magnetron structure and operating conditions suitable for long-pulse operation and phase-locking study. A large anode-cathode gap structure and a long washer cathode lower the electric field gradient and make long pulse, long lifetime operation possible. High vacuum ($10^{-7}$ Torr) environment and clean surface conditions are essential for long pulse rep-rated operation at 5 Hz.

## 5. ACKNOWLEDGEMENT

## 6. REFERENCE

1. S.C. Chen, G. Bekefi, and R.J. Temkin, "Operation of a long-pulse relativistic magnetron in a phase-locking system," H.E. Brandt, Editor, *Proc. SPIE*, vol. 1226, pp. 36-43, 1990.

2. S.C. Chen, G. Bekefi, R. Temkin, and C. de Graff, "Proposed injection locking of a long pulse relativistic magnetron," H.E. Brandt, Editor, *Proc. SPIE*, vol. 1061, pp. 157-160, 1989.

3. S.C. Chen and G. Bekefi, "Relativistic magnetron research," N. Rostoker, Editor, *Proc. SPIE*, vol. 873, pp 18-22, 1988.

4. J. Benford, H.M. Sze, W. Woo, R.R. Smith, and B. Harteneck, "Phase locking of relativistic magnetrons," *Phys. Rev Lett.*, vol. 62, pp. 969-971, 1989.

5. T.A. Treado, R.S. Smith III, C.S. Shaughnessy, and G.E. Thomas, "Temporal study of long-pulse relativistic magnetron operation", *IEEE Trans. on Plasma Science*, vol. 18, pp 594-602, 1990.

6. S.C. Chen "Growth and frequency pushing effects in relativistic magnetron phase-locking", *IEEE Trans. on Plasma Science*, vol. 18, pp 570-576, 1990.

7. G.L. Johnston, S.C. Chen, R.C. Davidson, and G. Bekefi, "Models of driven and mutually-coupled relativistic magnetrons with nonlinear frequency-shift and growth-saturation effects", H.E. Brandt, Editor, *Proc. SPIE*, vol. 1407 (in this volume), 1991.

8. G.L. Johnston, S.C. Chen, R.C. Davidson, and G. Bekefi, "Models of driven relativistic magnetrons with nonlinear frequency-shift and growth-saturation effects", H.E. Brandt, Editor, *Proc. SPIE*, vol. 1226, pp. 108-116, 1990.

9. W. Woo, J. Benford, D., Fittinghoff, B. Harteneck, D. Price, R. Smith, and H. Sze, "Phase locking of high-power microwave oscillators," *J. Appl. Phys.*, vol. 65, pp. 861-866, 1989.

10. W. Mulligan, S.C. Chen, G. Bekefi, B.G. Danly, and R.J. Temkin, "A high-voltage modulator for high-power rf source research", *IEEE Trans. on Elec. Dev.*, to be published in April, 1991.